De Novo Design of Nonpeptidic Compounds Targeting the Interactions between Interferon-α and its Cognate Cell Surface Receptor

Angelica M. Bello,[†] Tanushree Bende,[†] Lianhu Wei,[†] Xiaoyang Wang,[†] Beata Majchrzak-Kita,[†] Eleanor N. Fish,[†,‡,△] and Lakshmi P. Kotra*[,†,§,△,⊥]

Center for Molecular Design and Preformulations, Toronto General Research Institute, Toronto General Hospital, Toronto, ON M5G 2C4 Canada, Department of Immunology, Departments of Pharmaceutical Sciences and Chemistry, and McLaughlin Center for Molecular Medicine, University of Toronto, Toronto, Ontario, Canada, and Department of Chemistry and Biochemistry, The University of North Carolina at Greensboro, Greensboro, North Carolina 27412

Received September 19, 2007

Type 1 interferons (IFN) bind specifically to the corresponding receptor, IFNAR. Agonists and antagonists for IFNAR have potential therapeutic value in the treatment of viral infections and systemic lupus erythematosus, respectively. Specific sequences on the surface of IFN, IFN receptor recognition peptides (IRRPs) mediate the binding and signal transduction when IFN interacts with IFNAR. Structural features of two such IRRPs, IRRP-1 and IRRP-3, were used as templates to design small molecule mimetics. In silico screening was used to identify the molecular structural features mimicking their surface characteristics. A set of 26 compounds were synthesized and their ability to interfere with IFN−IFNAR interactions was investigated. Two compounds exhibited antagonist activity, specifically, blocking IFN-inducible Stat phosphorylation Stat complex-DNA binding. Design principles revealed here pave the way toward a novel series of small molecules as antagonists for IFN−IFNAR interactions.

Introduction

Interferons (IFNs[a]) are a family of biologically active proteins classified as type 1, type 2 and type 3.[1] Type 1 IFNs mediate diverse biological effects, including antiviral and antiproliferative responses, and several cell type-restricted responses of immunological relevance, such as maturation and differentiation of dendritic cells and modulation of B, T, and NK cell responses.[2] IFNs have widespread clinical application as therapeutic agents for the treatment of viral infections, especially in the context of hepatitis B and C (HBV and HCV) infections.[3] IFNs are clinically useful against a variety of solid tumors and hematological malignancies, including chronic myelogenous leukemia (CML), multiple myeloma, and hairy cell leukemia, and for the treatment of multiple sclerosis.[3–5] Deregulation of IFNs is implicated in certain autoimmune diseases such as systemic lupus erythematosus (SLE).[6–8]

Type 1 IFNs comprise a family of homologous helical bundle cytokines that in humans include 14 IFN-α subtypes and single IFN-β, IFN- κ, and IFN-ω subtypes. There is >50% sequence homology among all type-1 IFNs. IFNs α, β, ω, and κ activate the IFN receptor, IFNAR, engaging the two subunits of this receptor, IFNAR-1 and IFNAR-2.[9] Each of these subunits possesses a separate ligand-binding domain required for a functional ligand–receptor complex.[10,11] Mutational studies indicated that the binding of IFN-α and IFN-β elicits subtly different cellular responses, and the subunit IFNAR-2 is responsible for this differential recognition.[12,13] In recent years, the signaling events that follow IFN-α/β engagement of IFNAR have been extensively characterized.[14,15] Accumulating evidence suggests that distinct differences in critical amino acid residues among the different type-1 IFNs determine the nature of the ligand–receptor interaction and the subsequent responses.[10,14,16,17] At the outset, these interactions between IFN (the ligand) and IFNAR-1 and IFNAR2 (the receptor) domains may be characterized as protein–protein interactions. Due to the important roles that IFNs play (i) in protection from viral infections, in cancer, (ii) for their role in other autoimmune diseases, and (iii) cognizant that the potency of a particular IFN resides in the nature of the ligand–receptor interaction for individual IFNs,[11] we undertook a program of research to develop small molecule IFN mimetics, focusing on receptor interactive domains.

In the past several years, mimicking protein–protein interactions has attracted attention for therapeutics design.[18,19] Interfaces between protein–protein complexes are typically large and often flat surfaces, thus providing both opportunities and challenges for nonpeptidic molecular engineering.[20] Recently, we disclosed a de novo approach using in silico screening and designing novel scaffolds to target protein–protein interactions.[21] Here we outline a molecular approach involving in silico screening and a selection process to design a series of nonpeptidic pyrimidine based molecules that mimic targeted regions on the surface of the IFN molecule. It is anticipated that the compounds designed to bind to specific interactive subdomains in either IFNAR-1 or IFNAR-2 will compete and block the binding of IFN to the complete extracellular pocket described by IFNAR. Such molecules could be characterized as antagonists for IFN−IFNAR interactions. An ideal agonist will bind to and activate IFNAR. IFNAR antagonists will have potential utility in the treatment of autoimmune diseases such as systemic lupus erythematosus (SLE) and other diseases where IFN is implicated in pathogenesis. Design, synthesis, and functional assay results of this novel class of compounds are presented here, paving the way for the design of antagonists to IFNAR.

* Corresponding Author: Mailing address: #5-356, Toronto Medical Discoveries Tower/MaRS Center, 101 College Street, Toronto, Ontario, Canada M5G 1L7. Tel. (416) 581-7601, Fax . (416) 581-7621, E-mail: lkotra@uhnres.utoronto.ca.

[†] Toronto General Research Institute.

[‡] Department of Immunology, University of Toronto.

[§] Departments of Pharmaceutical Sciences and Chemistry, University of Toronto.

[△] McLaughlin Center for Molecular Medicine.

[⊥] The University of North Carolina at Greensboro.

[a] Abbreviations: IFN, interferon; IFNAR, interferon-α/β receptor; Stat, signal transducers and activator of transcription.

10.1021/jm701182y CCC: $40.75
Published on Web 04/05/2008

Scheme 1[a]

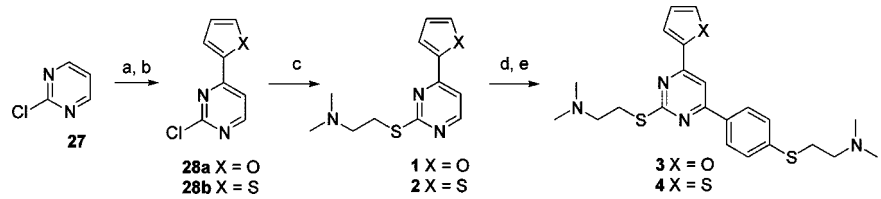

[a] Reagents and conditions: (a) furan or thiophene, *n*-BuLi, ether, −40 °C; (b) DDQ, NaOH; (c) NaOEt, reflux; (d) *n*-BuLi, ether, *N*,*N*-dimethyl-2[(4′-bromophenyl)thio]ethylamine, −40 °C; (e) DDQ, NaOH.

Experimental Section

Computer Modeling. An Octane2 workstation or a SGI Onyx3800 supercomputer was used to conduct in silico screening, visualization, and other computational tasks. Sybyl suite of software and Unity suite were used for database searches, comparisons, and other related tasks. Except when specified, default parameters and constraints were used in database searches.

Synthesis. General. All reactions involving air- or moisture-sensitive reagents were performed under nitrogen atmosphere. All solvents and reagents were obtained from commercial sources and dried using common procedures. Column chromatography was performed using 60 Å (70–230 mesh) silica gel. NMR spectra were recorded on a Varian spectrometer (300 or 400 MHz for ^{1}H; 75 or 100 MHz for ^{13}C). Chemical shifts are reported in δ ppm using tetramethylsilane as the reference. Mass spectra were determined in a Q-Star mass spectrometer using either ESI or EI technique. Purity of the compounds were established using Waters Delta 600 HPLC (symmetry C_{18}, 3.5 μm, 4.6 × 75 mm column), equipped with a 600 controller, and a 996 photodiode array detector using isocratic conditions (15 min; 0.5 mL/min flow rate; 60 to 100% 0.1% acetic acid in water/0–40% methanol). All solvents for HPLC were obtained from commercial sources and filtered through Waters membranes, 47 mm GHP 0.45 μm (Pall Corporation), and degassed with helium. Samples for HPLC were filtered through Waters Acrodisc syringe filters.

2-Chloro-4-(2-furyl) Pyrimidine (28a). Furan (15 mmol) was treated with *n*-butyl lithium (5 mmol) in anhyd diethyl ether at −40 °C for 30 min. Then a solution of 2-chloropyrimidine (4.5 mmol) in diethyl ether (10 mL) was added dropwise at −40 °C, and the resultant mixture was stirred at the same temperature for 1 h. The temperature of the reaction mixture was slowly allowed to rise to 0 °C and the stirring was continued for an additional hour. The reaction was quenched with water (0.5 mL) in THF (3 mL) and stirred for an additional 15 min. The reaction mixture was treated with DDQ (5 mmol) in THF (6 mL), stirred at room temperature for 25 min, and cooled in an ice bath. The reaction mixture was treated with hexanes (6 mL) and then with a cold solution of NaOH (3 M, 5 mL, 15 mmol) and stirred for 5 min. The organic layer was separated, washed with brine, and dried with anhyd Na_2SO_4. Solvent was evaporated to dryness and the residue was purified by column chromatography (hexanes/CH_2Cl_2) to yield **28a** (92% yield; Scheme 1).

2-Chloro-4-(2-thienyl) Pyrimidine (28b). This compound was synthesized from 2-chloropyrimidine (515 mg, 4.5 mmol) and thiophene (1.26 g, 15 mmol) using the procedure described for compound **28a**, and the product **28b** was isolated as a solid (832 mg, 94% yield; Scheme 1).

2-{[4-(2-Furyl)pyrimidin-2-yl]thio}-*N*,*N*-dimethylethanamine (1). Metallic sodium (120 mg, 5.2 mmol) was added to anhyd ethanol (10 mL), and the resulting solution of sodium ethoxide was treated with 2-(dimethylamino)ethanethiol hydrochloride (370 mg, 2.6 mmol). The mixture was stirred for 15 min at rt, then treated with compound **28a** (2 mmol), and stirred for an additional 12 h at 70 °C . The solvent was evaporated under vacuum, and the crude product was purified by column chromatography (hexanes/NEt_3/EtOH, 80:15:5) to obtain compound **1** as an oil (404 mg, 81%; Scheme 1).

***N*,*N*-Dimethyl-2-{[4-(2-thienyl)pyrimidin-2-yl]thio}ethanamine (2).** This compound was synthesized from **28b** (393 mg, 2 mmol) using the same method described for compound **1**. Yield: 451 mg, 85%. Hydrochloride salt was prepared using the method described for compound **1**.

2-({4-[2-{[2-(Dimethylamino)ethyl]thio}−6-(2-furyl)pyrimidin-4-yl]phenyl}thio)-*N*,*N*-dimethyl Ethanamine (3). Compound **3** was synthesized from compound **1** (500 mg, 2 mmol) and 2-(4-bromophenylthio)-*N*,*N*-dimethylethanamine (624 mg, 2.4 mmol) using the method described for compound **28a**, and the product was obtained in 72% yield (617 mg). Compound **3** (215 mg, 0.5 mmol) was dissolved in a small amount of methanol (1 mL). Then a solution of HCl in diethyl ether (3 mL, 1M) was added dropwise at 0 °C and the mixture was stirred for 30 min. Diethyl ether (20 mL) was added, and the precipitated solid was filtered and dried under vacuum to obtain the corresponding hydrochloride salt for compound **3**.

2-{[4-(4-{[2-(Dimethylamino)ethyl]thio}phenyl)-6-(2-thienyl)pyrimidin-2-yl]thio}-*N*,*N*-dimethyl Ethanamine (4). Starting from compound **2** (500 mg, 1.88 mmol) and *N*,*N*-dimethyl-2[(4′-bromophenyl)thio]ethylamine (588 mg, 2.26 mmol), compound **4** was synthesized using the method described for compound **28a**, with the final yield of 668 mg (76%).

General Method for the Synthesis of 31, 32, and 33 (Scheme 2). 2,4-Dichloro-6-ethoxypyrimidine (31a), 4,6-Dichloro-2-ethoxypyrimidine (32a), and 4-Chloro-2,6-diethoxypyrimidine (33a). Sodium (125 mg, 5.54 mmol) was dissolved in absolute ethanol (25 mL) at 0 °C and stirred for 15 min under argon. 2,4,6-Trichloropyrimidine **29** (1 g, 5.54 mmol) was added to the above reaction mixture and was stirred at the same temperature for an additional 24 h. Evaporation of the solvent and separation via column chromatography of the crude product produced compounds **31a** (821 mg, 78%), **32a** (160 mg, 15%), and minor **33a** (34 mg, 3%).

2,4-Dichloro-6-isopropoxypyrimidine (31b), 4,6-Dichloro-2-isopropoxyrimidine (32b), and 4-Chloro-2,6-diisopropoxypyrimidine (33b). Sodium (6.27 mg, 2.73 mmol) was dissolved in anhyd isopropanol (25 mL) at 0 °C and stirred for 15 min under argon. 2,4,6-Trichloropyrimidine **29** (500 mg, 2.73 mmol) was added to the above reaction mixture and was stirred at the same temperature for 24 h. Evaporation of the solvent and separation via column chromatography of the crude product produced compounds **31b** (428 mg, 76%), **32b** (108 mg, 19%), and **33b** (40 mg, 3%).

2,2′-[(6-Ethoxypyrimidine-2,4-diyl)bis(oxy)]bis(*N*,*N*-dimethylethanamine) (5). To a mixture of sodium (58 mg, 2.5 mmol) in anhyd THF (25 mL) was added an equivalent amount of *N*,*N*-dimethylethanolamine (223 mg, 2.5 mmol), and the solution was stirred at 0 °C. Then compound **31a** (193 mg, 1 mmol) dissolved in anhyd THF (5 mL) was added and continued stirring at 0 °C. After completion of the reaction, the solvent was evaporated under reduced pressure, and the residue was purified by column chromatography ($CHCl_3$/MeOH/Et_3N, 92:5:3) to afford compound **5** (275 mg, 92% yield).

2,2′-[(6-Isopropoxypyrimidine-2,4-diyl)bis(oxy)]bis(*N*,*N*-dimethylethanamine) (6). To a mixture of sodium (2.5 equiv) in anhyd THF (25 mL) was added an equivalent amount of *N*,*N*-dimethylethanolamine (2.5 equiv), and the solution was stirred at 0 °C. Then compound **31b** (1 equiv), dissolved in 5 mL of anhyd THF, was added and the stirring was continued at 0 °C. After the completion of the reaction, the solvent was evaporated and the

Scheme 2[a]

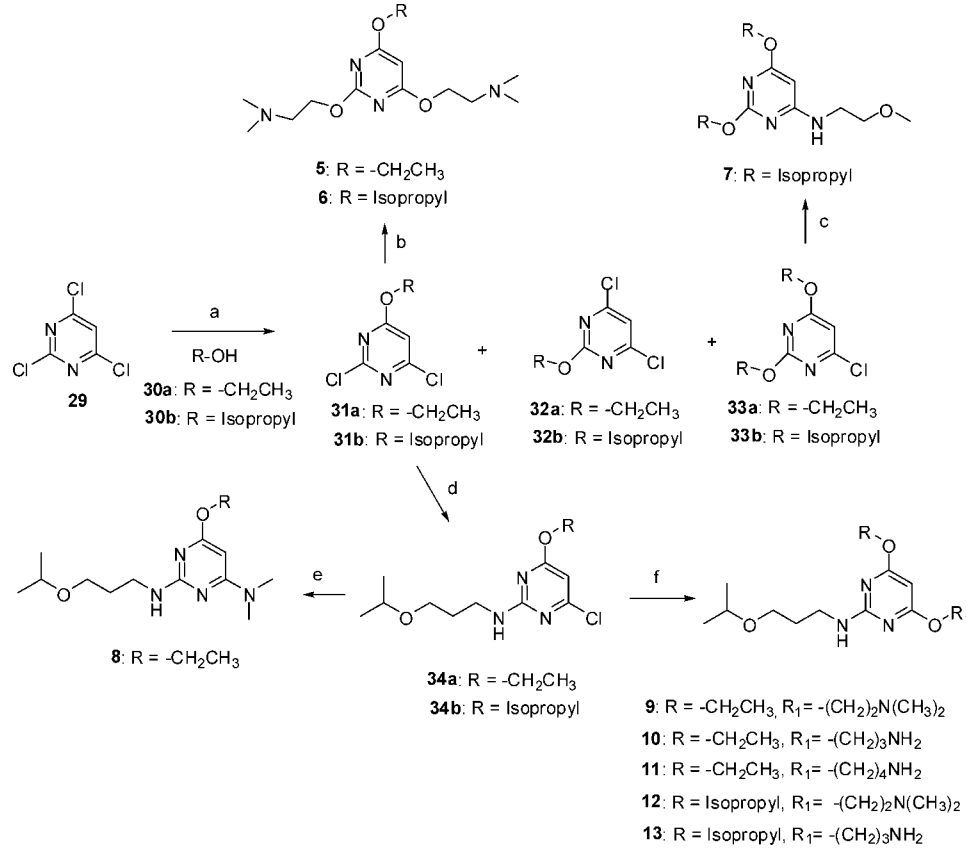

[a] Reagents and conditions: (a) sodium, 0 °C, 24 h; (b) *N*,*N*-dimethylethanolamine sodium, THF, 0 °C, 24 h; (c) 2-methoxyethylamine, THF, reflux; (d) isopropoxy propylamine, ethanol, Et_3N, 45 °C, 24 h; (e) Et_3N, DMF, 150 °C, 8 h; (f) NaH, Et_3N, ROH, THF, reflux, 14–24 h.

residue was purified by column chromatography ($CHCl_3$/MeOH/Et_3N = 92:5:3) to afford compound **6** (98%).

2,6-Diisopropoxy-*N*-(2-methoxyethyl)pyrimidin-4-amine (7). Compound **33b** (300 mg, 1.3 mmol) was dissolved in anhyd THF (5 mL) and 2-methoxyethylamine (293 mg, 3.9 mmol) was added. The reaction mixture was refluxed overnight. Evaporation of the solvent and the purification of the crude by column chromatography yielded compound **7** (339 mg, 97% yield).

4-Chloro-6-ethoxy-*N*-(3-isopropoxypropyl)pyrimidin-2-amine (34a). Compound **31a** (1 g, 5.18 mmol) and TEA (1 mL) were dissolved in anhyd ethanol (70 mL) and then 3-isopropoxypropylamine (1.75 g, 15 mmol) was added. The reaction mixture was stirred at 45 °C overnight. The solvent was evaporated under reduced pressure, and the residue was purified by chromatography (hexanes/$CHCl_3$/Et_2O = 5:5:1) to obtain compound **34a** as a white solid (1.23 g, 87%).

4-Chloro-6-isopropoxy-*N*-(3-isopropoxypropyl)pyrimidin-2-amine (34b). Compound **34b** was synthesized from compound **31a** (500 mg, 2.59 mmol) and isopropanol (50 mL) using the procedure followed for **34a**. Yield = 626 mg (84%).

6-Ethoxy-N^2-(3-isopropoxypropyl)-N^4,N^4-dimethylpyrimidine-2,4-diamine (8). A solution of compound **34a** (273 mg, 1 mmol) and triethylamine (1 mL) in DMF (20 mL) was stirred at 150 °C for 8 h. The reaction mixture was cooled to room temperature, and the solvent was evaporated under vacuum. The residue was taken in water (20 mL) and was extracted with ethyl acetate (3 × 20 mL). The combined organic layers were washed with brine (2 × 15 mL), dried (sodium sulfate), and concentrated under vacuum. The crude was purified by column chromatography (hexane/chloroform/diethyl ether = 2:2:1) to obtain compound **34a** as a syrup (180 mg, 64%).

4-(2-(Dimethylamino)ethoxy)-6-ethoxy-*N*-(3-isopropoxypropyl)pyrimidin-2-amine (9). *N*,*N*-Dimethylethanolamine (445 mg, 5 mmol) was added to a suspension of sodium hydride (60% dispersion in mineral oil, 200 mg, 5 mmol) in anhyd THF (5 mL) at 0 °C for 15 min. A solution of compound **34a** (274 mg, 1 mmol) and triethylamine (1 mL) in anhyd THF (15 mL) at 0 °C was slowly added, and the reaction mixture was refluxed overnight. After cooling to room temperature, the solution was quenched with cold water (10 mL) and extracted with ethyl acetate (3 × 20 mL). The combined organic layers were washed with brine (2 × 15 mL), dried with sodium sulfate, concentrated, and purified by column chromatography (EtOAc/MeOH/Et_2O/TEA = 10:1:3:1) to yield compound **9** as a pale yellow syrup (283 mg, 89%).

4-(3-Aminopropoxy)-6-ethoxy-*N*-(3-isopropoxypropyl)pyrimidin-2-amine (10). This compound was synthesized from **31a** (274 mg, 1 mmol) and 3-aminopropanol (375 mg, 5 mmol) using the procedure described for compound **9**. The crude product was purified by chromatography ($CHCl_3$/MeOH/TEA = 9:1:0.5) to obtain 283 mg (90% yield) product as pale yellow liquid.

4-(4-Aminobutoxy)-6-ethoxy-*N*-(3-isopropoxypropyl)pyrimidin-2-amine (11). This compound was synthesized from **31a** (274 mg, 1 mmol) and 4-amino-1-butanol (446 mg, 5 mmol) using the procedure described for compound **9**, and the reaction was refluxed for 20 h under nitrogen atmosphere. The crude product was purified by column chromatography ($CHCl_3$/MeOH/Et_3N = 9:1:0.5) to obtain compound **11** as a pale yellow syrup (150 mg, 46%).

4-(2-(Dimethylamino)ethoxy)-6-isopropoxy-*N*-(3-isopropoxypropyl)pyrimidin-2-amine (12). This compound was synthesized from **31b** (288 mg, 1 mmol) and *N*,*N*-dimethylethanolamine (445 mg, 5 mmol) using the procedure described for compound **9**, and the reaction was refluxed for 24 h under nitrogen atmosphere. The crude product was purified by column chromatography ($CHCl_3$/MeOH/TEA = 9:1:0.5) to obtain compound **12** as a pale yellow liquid (302 mg, 89%).

4-(3-Aminopropoxy)-6-isopropoxy-*N*-(3-isopropoxypropyl)pyrimidin-2-amine (13). This compound was synthesized from **31b** (288 mg, 1 mmol) and 3-aminopropanol (375 mg, 5 mmol) using

Scheme 3[a]

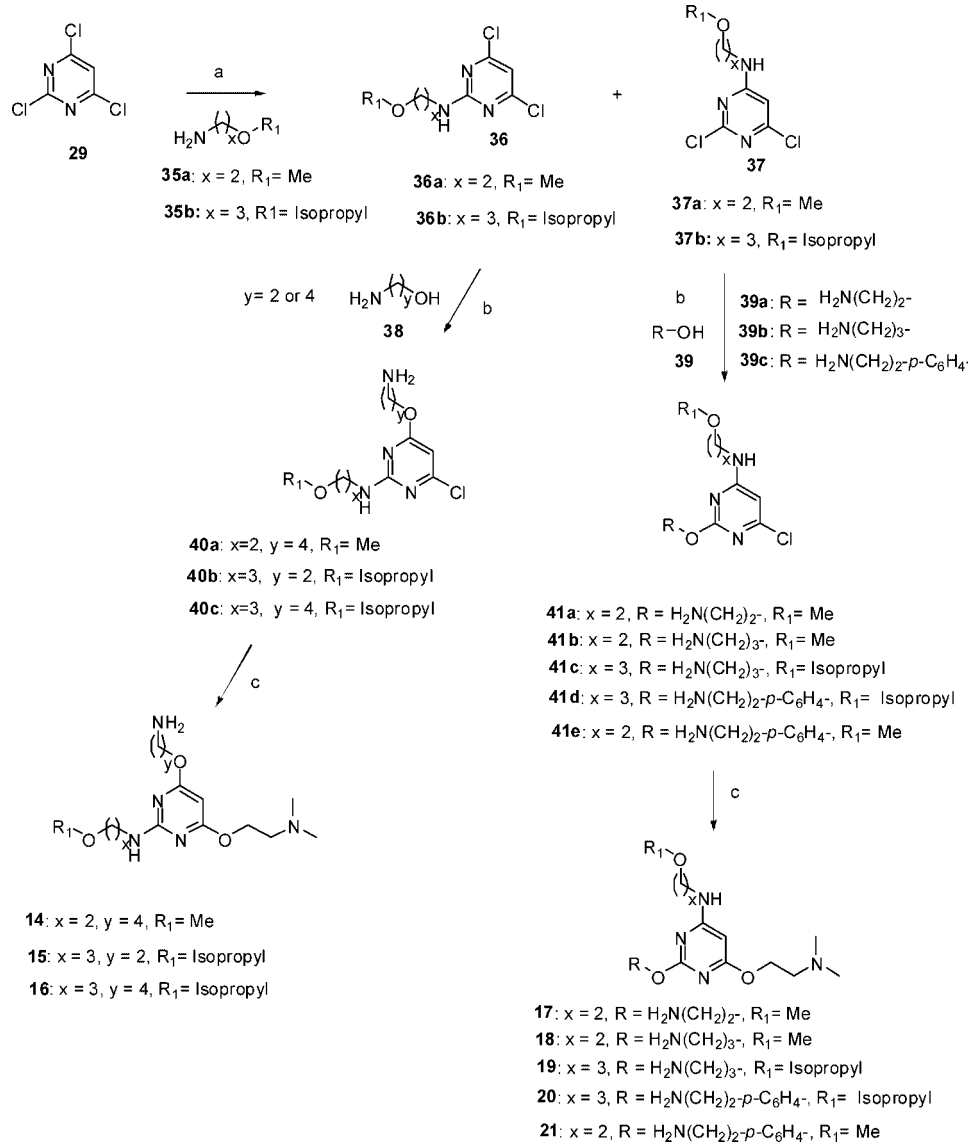

[a] Reagents and conditions: (a) EtOH, 40 °C, 24 h; (b) NaH, THF, DIEA, 40 °C, 20 h; (c) NaH, THF, *N*,*N*-dimethylethanolamine, 0.3 equiv of DIEA, 60 °C, 24 h.

the procedure described for compound **9**. The product was isolated as a pale yellow liquid (280 mg, 86%).

General Method for the Synthesis of 36 and 37 (Scheme 3). 4,6-Dichloro-*N*-(2-methoxyethyl)pyrimidin-2-amine (36a) and 2,6-Dichloro-*N*-(2-methoxyethyl)pyrimidin-4-amine (37a). To a solution of 2,4,6-trichloropyrimidine **29** (7 g, 38.1 mmol) in 15 mL of anhyd ethanol, 2-methoxyethanamine **35a** (2.861 g, 38.1 mmol) was added. The reaction mixture was stirred at 40 °C for 24 h, and then the solvent was removed under reduced pressure. The crude product was purified by column chromatography (hexane/EtOAc, 9:1) to obtain compound **36a** (4.89 g, 58%) and compound **37a** (2.54 g, 30%) as a white solid.

4,6-Dichloro-*N*-(3-isopropoxypropyl)pyrimidin-2-amine (36b) and 2,6-Dichloro-*N*-(3-isopropoxypropyl)pyrimidin-4-amine (37b). This compound was synthesized from 2,4,6-trichloropyrimidine **29** (7 g, 38.1 mmol) and 3-isopropoxypropan-1-amine **35b** (4.462 g, 38.1 mmol) by the method described for compound **36a** and **37a**. Compound **36b**: white solid (5.91 g, 59%); compound **37b**: white solid (3.13 g, 31%).

General Procedure for the Synthesis of Compounds 40a−40c and 41a−41e (Scheme 3). 4-(4-Aminobutoxy)-6-chloro-*N*-(2-methoxyethyl)pyrimidin-2-amine (40a). To an ice-cooled solution of 4-amino-1-butanol **38** ($y = 4$; 337 mg, 3.78 mmol) in anhyd THF (2 mL), sodium hydride (166 mg, 4.15 mmol; 60% dispersion in mineral oil) was added, and the mixture was stirred for 15 min at 0 °C. Then 4,6-dichloro-*N*-(2-methoxyethyl)pyrimidin-2-amine **36a** (840 mg, 3.78 mmol) and a catalytic amount of DIEA (0.13 mL, 0.756 mmol) were added, and the mixture was stirred at 40 °C for 20 h under a nitrogen atmosphere. The reaction mixture was quenched with saturated aqueous ammonium chloride solution, extracted with ethyl acetate (3 × 15 mL) and the combined organic layers were washed with brine. The organic phase was dried over anhyd sodium sulfate and concentrated under vacuum. The residue was purified by column chromatography (silica gel) using a gradient elution ($CHCl_3$/MeOH/TEA 99:0:1→97:2:1) to afford compound **40a** as a pale yellow liquid (727 mg, 70%).

4-(2-Aminoethoxy)-6-chloro-*N*-(3-isopropoxypropyl)pyrimidin-2-amine (40b). Compound **40b** was synthesized from 4,6-dichloro-*N*-(3-isopropoxypropyl)pyrimidin-2-amine **36b** (1 g, 3.78 mmol) and 2-aminoethanol **38** ($y = 2$; 231 mg, 3.78 mmol) using the procedure described for compound **40a**. Yield: 655 mg, 69%.

4-(4-Aminobutoxy)-6-chloro-*N*-(3-isopropoxypropyl)pyrimidin-4-amine (40c). Compound **40c** was synthesized from 4,6-dichloro-*N*-(3-isopropoxypropyl)pyrimidin-2-amine **36b** (1 g, 3.78 mmol) and 4-aminobutan-1-ol **38** ($y = 4$; 337 mg, 3.78 mmol) using the procedure described for compound **40a**. Yield: 982 mg, 82%.

2-(2-Aminoethoxy)-6-chloro-*N*-(2-methoxyethyl)pyrimidin-4-amine (41a). Compound **41a** was synthesized from 2,6-dichloro-*N*-(2-methoxyethyl)pyrimidin-4-amine **37a** (1 g, 4.5 mmol) and 2-aminoethanol **39a** (275 mg, 4.5 mmol) using the procedure described for compound **40a**. Yield: 720 mg, 65%.

2-(3-Aminopropoxy)-6-chloro-*N*-(2-methoxyethyl)pyrimidin-4-amine (41b). Compound **41b** was synthesized from 2,6-dichloro-*N*-(2-methoxyethyl)pyrimidin-4-amine **37a** (1 g, 4.5 mmol) and 3-amino-1-propanol **39b** (338 mg, 4.5 mmol) using the procedure described for compound **40a**. Yield: 850 mg, 72%.

2-(3-Aminopropoxy)-6-chloro-*N*-(3-isopropoxypropyl)pyrimidin-4-amine (41c). Compound **41c** was synthesized from 2,6-dichloro-*N*-(3-isopropoxypropyl)pyrimidin-4-amine **37b** (1 g, 3.78 mmol) and 3-amino-1-propanol **39b** (284 mg, 3.78 mmol) using the procedure described for compound **40a**. Yield: 810 mg, 71%.

2-[4-(2-Aminoethyl)phenoxy]-6-chloro-*N*-(3-isopropoxypropyl) pyrimidin-4-amine (41d). Compound **41d** was synthesized from 2,6-dichloro-*N*-(3-isopropoxypropyl)pyrimidin-4-amine **37b** (280 mg, 1.06 mmol) and 4-(2-aminoethyl)phenol **39c** (145 mg, 1.06 mmol) using the procedure described for compound **40a**. Yield: 240 mg, 62%.

2-[4-(2-Aminoethyl)phenoxy]-6-chloro-*N*-(2-methoxyethyl)pyrimidin-4-amine (41e). Compound **41d** was synthesized from 2,6-dichloro-*N*-(2-methoxyethyl)pyrimidin-4-amine **37a** (378 mg, 1.70 mmol) and 4-(2-aminoethyl)phenol **39c** (233 mg, 1.70 mmol) using the procedure described for compound **40a**. Yield: 380 mg, 69%.

General Procedure for the Synthesis of Compounds 14–21 (Scheme 3). 4-(4-Aminobutoxy)-6-(2-(dimethylamino)ethoxy)-*N*-(2-methoxyethyl)pyrimidin-2-amine (14). Sodium hydride (360 mg, 9 mmol, 60% dispersion in mineral oil) was added to an ice-cooled solution of *N*,*N*-dimethylethanolamine (802 mg, 9 mmol) in anhyd THF (15 mL), and the mixture was stirred for 30 min at 0 °C. Then 4-(4-aminobutoxy)-6-chloro-*N*-(2-methoxyethyl)pyrimidin-2-amine **40a** (495 mg, 1.8 mmol) and a catalytic amount of DIPEA (0.1 mL, 0.5 mmol) were added, and the mixture was stirred at 60 °C for 24 h under a nitrogen atmosphere. The reaction mixture was quenched with saturated aqueous NH_4Cl solution, and the crude was extracted with ethyl acetate (3 × 20 mL). The combined ethyl acetate layers were washed with brine (15 mL), dried over anhyd sodium sulfate, and concentrated under vacuum. The residue was purified on a silica gel column chromatography using gradient elution with $CHCl_3$/MeOH/TEA (97:0:3 to 92:4:4) to yield compound **14** as a light yellow liquid (420 mg, 71%). Compound **14** was converted into its hydrochloride salt following the method described for the hydrochloride salt of compound **3**.

4-(2-Aminoethoxy)-6-(2-(dimethylamino)ethoxy)-*N*-(3-isopropoxypropyl)pyrimidin-2-amine (15). Compound **15** was synthesized from 4-(2-aminoethoxy)-6-chloro-*N*-(3-isopropoxypropyl)pyrimidin-2-amine **40b** (491 mg, 1.70 mmol) and *N*,*N*-dimethylethanol amine (758 mg, 8.5 mmol) using the procedure described for compound **14**. Yield: 380 mg, 65%.

4-(4-Aminobutoxy)-6-[2-(dimethylamino)ethoxy]-*N*-(3-isopropoxypropyl)pyrimidin-4-amine (16). Compound **15** was synthesized from 4-(4-aminobutoxy)-6-chloro-*N*-(3-isopropoxypropyl)pyrimidin-2-amine **40c** (500 mg, 1.6 mmol) and *N*,*N*-dimethylethanol amine (713 mg, 8 mmol) using the procedure described for compound **14**. Yield: 0.384 g, 66%.

2-(2-Aminoethoxy)-6-(2-(dimethylamino)ethoxy)-*N*-(2-methoxyethyl)pyrimidin-4-amine (17). Compound **17** was synthesized from 2-(2-aminoethoxy)-6-chloro-*N*-(2-methoxyethyl)pyrimidin-4-amine **41a** (493 mg, 2 mmol) and *N*,*N*-dimethylethanol amine (890 mg, 10 mmol) using the procedure described for compound **14**. Yield: 380 mg, 64%.

2-(3-Aminopropoxy)-6-(2-(dimethylamino)ethoxy)-*N*-(2-methoxyethyl)pyrimidin-4-amine (18). Compound **18** was synthesized from 2-(3-aminopropoxy)-6-chloro-*N*-(2-methoxyethyl)pyrimidin-4-amine **41b** (495 mg, 1.9 mmol) and *N*,*N*-dimethylethanol amine (847 mg, 9.5 mmol) using the procedure described for compound **14**. Yield: 470 g, 79%.

2-(3-Aminopropoxy)-6-(2-(dimethylamino)ethoxy)-*N*-(3-isopropoxypropyl)pyrimidin-4-amine (19). Compound **19** was synthesized from 2-(3-aminopropoxy)-6-chloro-*N*-(3-isopropoxypropyl)pyrimidin-4-amine **41c** (430 mg, 1.42 mmol) and *N*,*N*-dimethylethanol amine (633 mg, 7.1 mmol) using the procedure described for compound **14**. Yield: 480 mg, 82%.

Scheme 4[a]

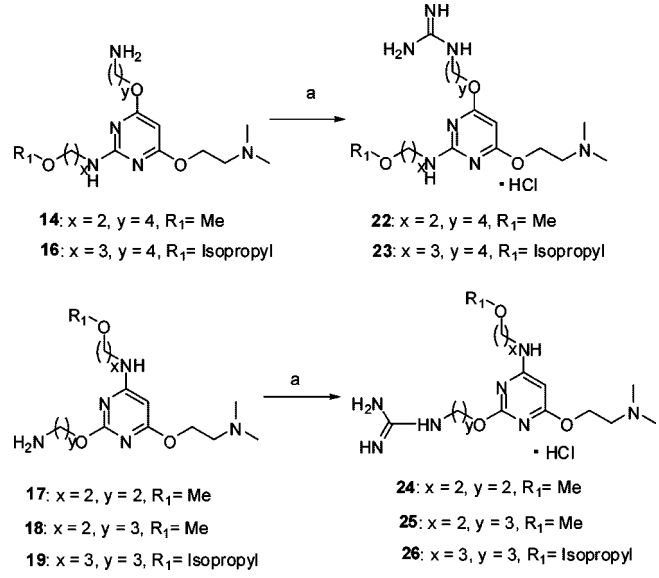

[a] Reagents and conditions: (a) 1*H*-pyrazole-1-carboxamidine·HCl/DIEA, rt, 40 h.

2-(4-(2-Aminoethyl) phenoxy)- 6-(2-(dimethylamino)ethoxy)-*N*-(3-isopropoxypropyl)pyrimidin-4-amine (20). Compound **20** was synthesized from 2-(4-(2-aminoethyl)phenoxy)-6-chloro-*N*-(3-isopropoxypropyl)pyrimidin-4-amine **41d** (183 mg, 0.5 mmol) and *N*,*N*-dimethylethanol amine (223 mg, 2.5 mmol) using the procedure described for compound **14**. Yield: 120 mg, 56%.

2-(4-(2-Aminoethyl)phenoxy)-6-(2-(dimethylamino)ethoxy)-*N*-(2-methoxyethyl)pyrimidin-4-amine (21). Compound **21** was synthesized from 2-(4-(2-aminoethyl)phenoxy)-6-chloro-*N*-(2-methoxyethyl)pyrimidin-4-amine **41e** (130 mg, 0.4 mmol) and *N*,*N*-dimethylethanolamine (178 mg, 2 mmol) using the procedure described for compound **14**. Yield: 90 mg, 61%.

General Procedure for the Synthesis of Compounds 22–26 (Scheme 4). 1-(4-(6-(2-(Dimethylamino)ethoxy)-2-(2-methoxyethylamino)pyrimidin-4-yloxy)butyl)guanidine Hydrochloride (22). 4-(4-Aminobutoxy)-6-(2-(dimethylamino)ethoxy)-*N*-(2-methoxyethyl)pyrimidin-2-amine **16** (50 mg, 0.15 mmol) was dissolved in DMF (2 mL) and was treated with 1*H*-pyrazole-1-carboxamidine·HCl (23 mg, 0.16 mmol) and DIEA (27 μL, 0.16 mmol). The reaction mixture was stirred at room temperature under nitrogen for 40 h. Solvent was evaporated under reduced pressure, and the crude product was washed with several portions of ether and dried. The crude product was recrystallized from MeOH/ether to obtain compound **22** as a white solid (44 mg, 72%).

1-(4-(6-(2-(Dimethylamino)ethoxy)-2-(3-isopropoxypropylamino)pyrimidin-4-yloxy)butyl)guanidine Hydrochloride (23). Compound **23** was synthesized from 4-(4-aminobutoxy)-6-(2-(dimethylamino)ethoxy)-*N*-(3-isopropoxypropyl)pyrimidin-2-amine **14** (50 mg, 0.13 mmol) and 1*H*-pyrazole-1-carboxamidine·HCl (23 mg, 0.16 mmol) using the procedure described for compound **22**. Yield: 46 mg, 82%.

1-(2-(4-(2-(Dimethylamino)ethoxy)-6-(2-methoxyethylamino)pyrimidin-2-yloxy)ethyl)guanidine Hydrochloride (24). Compound **24** was synthesized from 2-(2-aminoethoxy)-6-(2-(dimethylamino)ethoxy)-*N*-(2-methoxyethyl)pyrimidin-4-amine **17** (45 mg, 0.15 mmol) and 1*H*-pyrazole-1-carboxamidine·HCl (23 mg, 0.16 mmol) using the procedure described for compound **22**. Yield: 45 mg, 80%.

1-(3-(4-(2-(Dimethylamino)ethoxy)-6-(2-methoxyethylamino)pyrimidin-2-yloxy)propyl)guanidine Hydrochloride (25). Compound **25** was synthesized from 2-(3-aminopropoxy)-6-(2-(di-

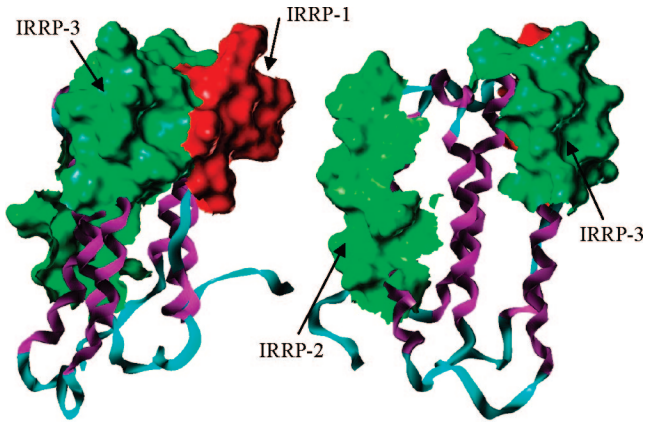

Figure 1. Ortho view of the structure of IFN-α2a (pdb: 1ITF). The IRRP regions are illustrated as a Connolly surface: IRRP-1 (residues 29–35), IRRP-2 (residues 78–95), and IRRP-3 (residues 123–140) are depicted in red, green, and blue-green, respectively.

methylamino)ethoxy)-*N*-(2-methoxyethyl)pyrimidin-4-amine **18** (45 mg, 0.14 mmol) and 1*H*-pyrazole-1-carboxamidine·HCl (23 mg, 0.16 mmol) using the procedure described for compound **22**. Yield: 48 mg, 85%.

1-(3-(4-(2-(Dimethylamino)ethoxy)-6-(3-isopropoxypropyl)amino)pyrimidin-2-yloxy)propyl)guanidine Hydrochloride (26). Compound **26** was synthesized from 2-(3-aminopropoxy)-6-(2-(dimethylamino)ethoxy)-*N*-(2-methoxyethyl)pyrimidin-4-amine **19** (45 mg, 0.13 mmol) and 1*H*-pyrazole-1-carboxamidine·HCl (23 mg, 0.16 mmol) using the procedure described for compound **22**. Yield: 48 mg, 87%.

Design Strategy. The strategy for the design of IFN mimics to create small molecule antagonists considered (i) the availability of hot spot regions on IFN-α, (ii) the availability of the three-dimensional structures of IFNs-α/β, and (iii) the possibility to map small molecules onto the hot spot regions on the IFN.[12,13,22,23] Site-directed mutagenesis studies further identified three regions of conserved residues among IFN-αs, the AB-loop spanning Cys29-Phe36 (AB domain), the helix C spanning Glu78-Asp95 (C domain), and the helix D along with the adjacent DE loop spanning Tyr122-Ala139 (D domain), as functionally important regions interacting with the IFNAR.[14,24] These three regions are labeled as IRRP-1, IRRP-2, and IRRP-3, respectively (IRRP = interferon receptor recognition peptide). When IRRPs are mapped onto the X-ray structure of IFN-α2a, these regions concentrate on two sides of the protein (Figure 1).[16,23,25] The solvent accessible surface areas of IRRP-1, IRRP-2, and IRRP-3 are 457, 839, and 865 Å^2, respectively. Each face of the IFN binds to one subdomain of IFNAR: IRRP-1 and IRRP-3 bind to an IFNAR2 subdomain and the IRRP-2 region binds to an IFNAR-1 subdomain.[11] Productive interactions with both IFNAR1 and IFNAR2 are essential for a molecule to function as an agonist. However, for an antagonist, it would suffice to bind to either IFNAR1 or IFNAR2 such that an IFN molecule cannot productively bind to both receptor subdomains to activate the receptor and elicit a biological response.[11] We initially targeted the regions of IRRP-1 and IRRP-3 as the templates to mimic on the surface of IFN. Because these two IRRPs are contiguous and bind to the IFNAR2 portion of the receptor, molecules mimicking either of these IRRPs are anticipated to interfere with IFN-inducible receptor-mediated activities. In other words, such small molecules would be antagonists at the IFNAR.

The three-dimensional structure of the IRRP-1 region in IFN-α2a was used as a template to perform the molecular design. Based on the structural analyses of the IRRP-1 segment, four residues were chosen as the key mimicry residues. These are the hydrophobic side chain of Leu30, the hydrophobic aromatic side chain on His34, and the positively charged groups on Lys31 and Arg33. The midpoint between the atoms CD1 and CD2 on the residue Leu30 and the center of the imidazole ring of His34 were defined as

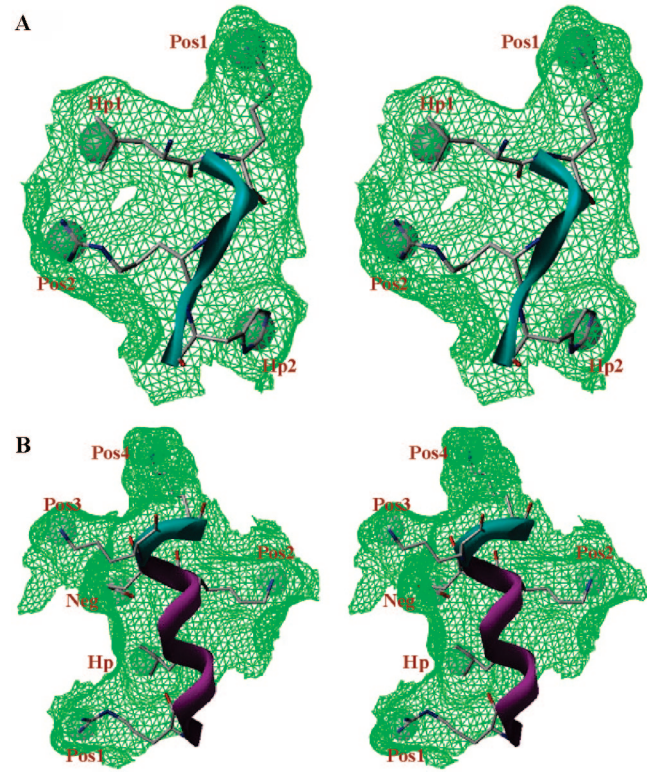

Figure 2. Stereoview of the structural features on surface of human IFN-α2a used in the in silico screens targeting IRRP-1 and IRRP-3 regions (panels A and B, respectively). Amino acids are shown in capped-stick models. Grey spheres represent the centers of each selected feature. Connolly surface is depicted as a mesh in green and the backbone of the interferon is shown as a ribbon.

hydrophobic centers (Hp1 and Hp2, respectively); Nζ of the residue Lys31 and the midpoint between NH1 and NH2 atoms in the residue Arg33 were defined as the positively charged centers (Pos1 and Pos2, respectively; Figure 2A). An in silico database search using UNITY suite of software was performed using the above definition for the molecular search against three databases, with a total of over 300000 molecules: the NCI database, the Maybridge database, and the LeadQuest database.[26] The search criteria included the identification of the hit molecules matching at least three of the four features (Hp1, Hp2, Pos1, and Pos2). A distance tolerance of 1 Å was set between any two features and a tolerance of 1 Å was set as a volume constraint. In the first filtration process, 1010 compounds were selected that satisfy the above criteria. These molecules were further screened for their molecular complexity and synthetic feasibility. Finally, three compounds **42** (NCI-119030), **43** (1502–09435), and **44** (CD11398) were identified from the above in silico filtration process (Figure 3A,C).[27] These molecules were further refined and arrived at the focused library featuring compounds **5**−**26** represented by species II in Figure 4C.

Another in silico search targeting IRRP-3 was initiated to design a second small molecule mimicking this region. IRRP-3 on human IFN-α2a spans the residues 122–139. Side chains from six residues, namely, Arg125, Leu128, Lys131, Glu132, Lys133, and Lys134, were used as the hot spot regions for the mimicry of IRRP-3. Based on the structural features of these six residues on the surface of IFN-α2a, the following structural features were selected for the in silico search: the midpoint between the atoms NH1 and NH2 of the residue Arg125, Nϵ atoms in Lys131, Lys133, and Lys134 (designated as Pos1, Pos2, Pos3, and Pos4, respectively); additionally, the midpoint between the atoms CD1 and CD2 on the residue Leu128 (designated as Hp) and the midpoint between OE1 and OE2 on the residue Glu132 (designated as Neg) were assigned as hydrophobic and negatively charged centers, respectively (Figure 2B). These six regions were selected on the basis of their position

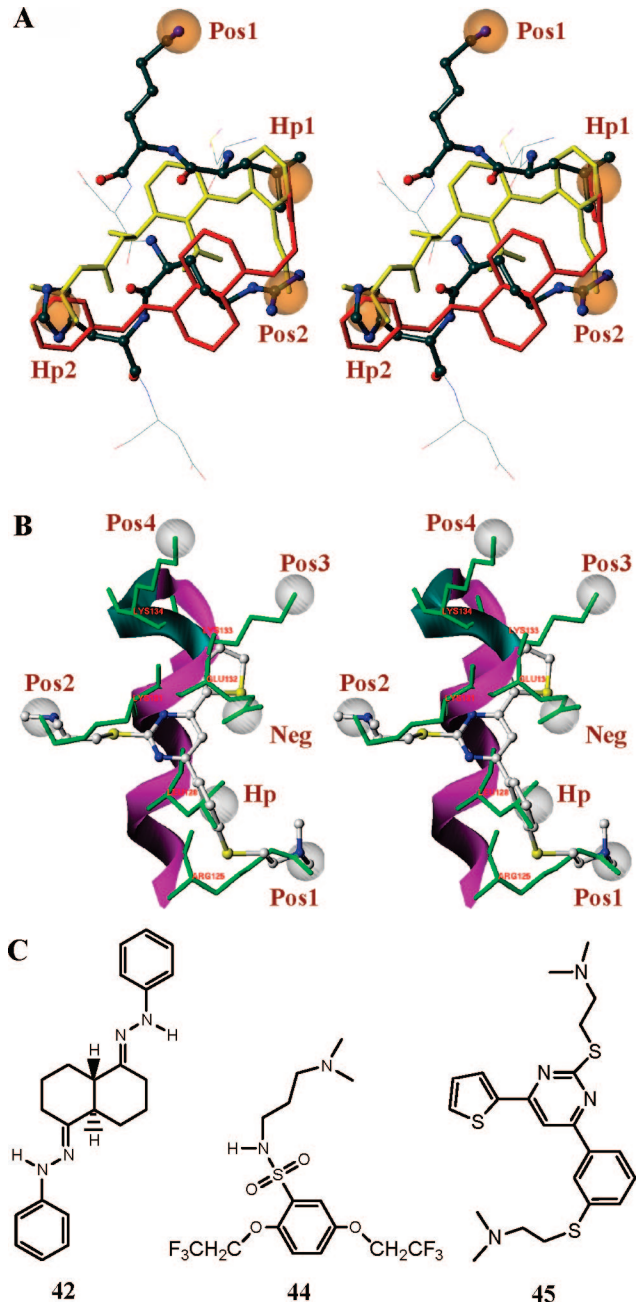

Figure 3. (A) Stereoview of the overlap of IRRP-1 region and the two hits **42** (in red) and **43** (in yellow) identified from the chemical databases search. Orange spheres represent the search criteria based on the structure of IRRP-1: sphere at 12 o'clock represents a cationic moiety (Pos1), at 3 o'clock represents a hydrophobic moiety (Hp1), at 4 o'clock represents the second cationic moiety (Pos2), and at 6 o'clock represents the second hydrophobic moiety (Hp2). (B) Stereoview of the overlap of **45** onto the IRRP-3 segment of IFN-α2a. The backbone of the protein is shown as a ribbon in magenta, the residues of IRRP-3 are shown in green in capped stick representation, and **45** is shown in ball-and-stick representation color-coded according to atom type. White spheres represent the six functional regions that were used in in silico database search. (C) Chemical structures of **42**, **44**, and **45**.

exposed to the solvent and their hydrophobic/electronic charge characteristics. A distance tolerance of 1 Å was set between any two features and a tolerance of 1 Å was set as a volume constraint. A total of 192 compounds were identified from the three databases matching at least three of the six features used from the IRRP-3 region. These compounds were further screened manually for their chemical nature, feasibility of synthesis, and/or druggability features, ultimately selecting one molecule **45** (NCI-619009) as a "hit" structure targeting IRRP-3 (Figure 3B,C).[28] Thus, a small set of compounds **1**–**4** were designed to evaluate the potential of this designed core mimicking IRRP-3. Below, chemical synthesis for all the designed compounds, **1**–**26** is outlined.

In Vitro Activity Evaluation. Two series of experiments were conducted to evaluate the antagonistic effects of the designed compounds **1**–**26** on IFN-inducible events. First, all compounds (100 μm) were screened for their inhibitory effects on IFN-induced Stat-1 tyrosine phosphorylation. Next, we examined their ability to interfere with IFN-inducible Stat complex formation and DNA binding. Daudi cells were either left untreated or treated with IFN (100 pg) for 15 min in the presence or absence of the target compounds, as indicated. Cell lysates were then prepared and resolved by SDS-PAGE, and the proteins were transferred to nitrocellulose and immunoblotted (WB) for phospho-Stat1, using standard protocols.[29] The membranes were stripped and were reprobed for Stat1. Alternatively, β-actin was used as loading control.

For the evaluation of Stat1 complex formation, Daudi cells were either left untreated or treated with IFN in the presence or absence of compounds for 15 min. Nuclear extracts from these cells were prepared, mixed with a ^{32}P-labeled palindromic IFN-responsive element (^{32}P-pIRE) probe to assess IFN-inducible Stat1:Stat1 and Stat1:Stat3 dimer formation and DNA binding, and resolved by native agarose gel electrophoresis.[30] Only those compounds that showed potential inhibition of IFN activity in the Stat1 phosphorylation assay were subjected to this radiolabeled electrophoretic mobility shift assay (EMSA) to further confirm their inhibitory activities.

Results and Discussion

Chemistry. Compounds **1**−**4** were synthesized according to Scheme 1. Either furan (for compounds **1** and **3**) or thiophene (for **2** and **4**) were added to 2-chloropyrimidine after activation with *n*-butyl lithium. The crude products were subjected to oxidation by the treatment with DDQ to yield **28a** and **28b**.[31] Compounds **1** and **2** were obtained by nucleophilic substitution of chlorine on **28a** and **28b** by *N*,*N*-(dimethylamino)ethanethiol in the presence of metallic sodium, respectively.[32] Compounds **1** and **2** were further substituted at position 6 by the addition-dehydrogenation using lithiated *N*,*N*-dimethyl-2[(4′-bromophenyl)thio]ethylamine followed by the treatment with DDQ to yield compounds **3** and **4**.[33]

The substituted pyrimidines **5**−**13** were synthesized starting from 2,4,6-trichloropyrimidines (Scheme 2). 2,4,6-Trichloropyrimidine was first treated with an appropriate alkoxide to obtain 2- and 4-monosubstituted derivatives, as well as a small amount of 2,4-disubstituted derivative. These regioisomers were separated by silica gel column chromatography. Subsequent treatment of 4-alkoxy pyrimidine derivative (**31a** and **31b**) with isopropoxy propylamine in the presence of ethanol and triethylamine led to the regioselective substitution at position 2 yielding **34a** and **34b**. Treatment of compounds **31a** and **31b** with *N*,*N*-dimethylethanolamine yielded compound **5** and **6**, respectively. Treatment of **33b** with 2-methoxyethylamine in THF under refluxing conditions provided access to compound **7**. Substitution with various alkoxides in the presence of triethyl amine afforded the substitution at 6-position to obtain the final pyrimidine derivatives **8**−**13**.

Compounds **14**−**21** were synthesized using the protocols in Scheme 3 starting from 2,4,6-trichloropyrimidine. When compound **29** was treated with an alkoxyamine (methoxy and isopropyloxy derivatives), regioisomers **36** and **37** were isolated in 2:1 ratio. These two regioisomers were separated and were further treated with various aminoalkoxides in presence of diisopropylethylamine at 40 °C to afford regioselective substitution at 4- and 2-positions on **36** and **37** to yield compounds

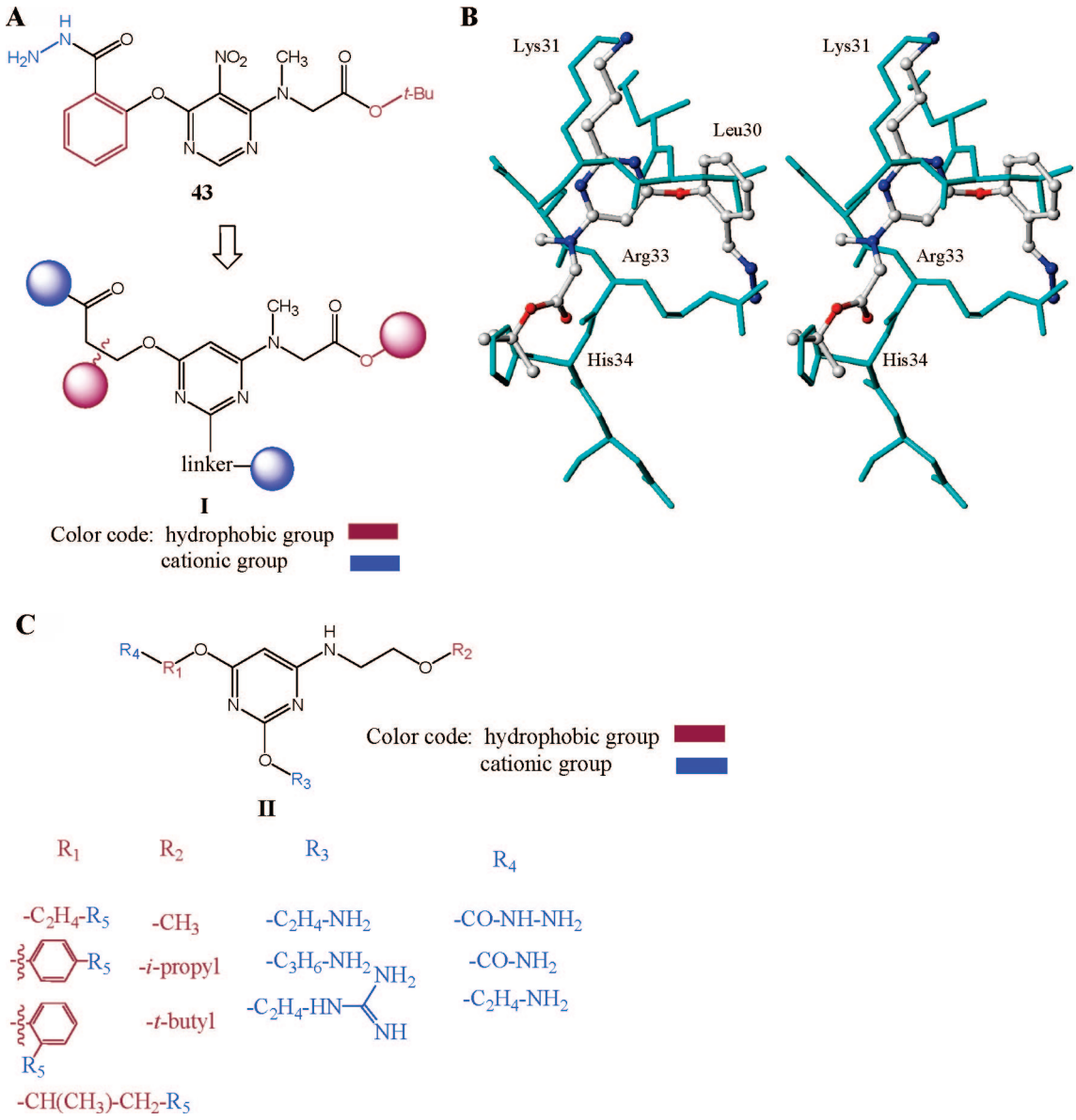

Figure 4. (A) Schematic of compound **43** and its morphosis into species I mimicking IRRP-1 interactions. (B) Stereoview of the overlap of a model compound onto the IRRP-1 segment of IFN-α2a. IRRP-1 residues are in cyan and species II is shown as a ball-and-stick model. (C) Chemical library based on general scaffold I (also see Scheme 1).

40a−**c** and **41a**−**e**, respectively. Nucleophilic substitution at the 6-position on compounds **40a**−**c** and **41a**−**e** was carried out with the appropriate aminoalkoxide at 60 °C in the presence of sodium hydride and DIEA to afford the target compounds **14**−**21**. A remarkable increase in the yields was observed when proton scavengers such as diisopropyl ethylamine or triethyl amine were used in THF as a solvent rather than DMF, which produced lower yields and side products. Guanidinylation of the primary amine derivatives **14**, **16**–**19** was achieved by using pyrazole-1-carboxamidine under basic conditions to yield compounds **22**−**26**.[34] All designed compounds **1**–**26** were confirmed for their purity for subsequent biological activity evaluations.

This effort started with the hypothesis that one could mimic the "functional hot spots" on the surface of the protein–ligand IFN-α2a using small molecules. While the design principles for agonist activity due to such small molecules could be quite complicated, it was envisioned that (i) mimics of smaller regions of the surface of IFN-α2a could be feasible and (ii) such small molecules would interfere with the binding of this ligand at its receptor. Such molecules would most likely exhibit the antagonist activity. The above synthesized two series of compounds, namely, **1**–**26** were evaluated for their ability to competitively inhibit IFN in the cell-based assays.

Activation of the IFNAR that results in comprehensive signal transduction requires that both IFNAR1 and IFNAR2 be activated, for example, the ligand has to interact with both subdomains.[11] This activation involves the phosphorylation-activation of IFNAR2- and IFNAR1-associated kinases, Jak1 and Tyk2, respectively, then the phosphorylation of the intracellular domains of the receptor subunits on specific tyrosine residues by these kinases. This results in the recruitment of Stat proteins to the receptor and their phosphorylation-activation, specifically the Stat proteins Stat1, Stat2, Stat3, and Stat5. Once phosphorylated, Stats will form complexes: Stat1:Stat1, Stat1:Stat3, Stat3:Stat3, Stat2:Stat1/IRF-9, and Stat5:CrkL. These activated Stat complexes translocate to the nucleus where they bind to specific target elements in the promoters of IFN sensitive genes, thereby activating their transcription. IFN-sensitive genes mediate the different IFN-inducible biological responses.[35]

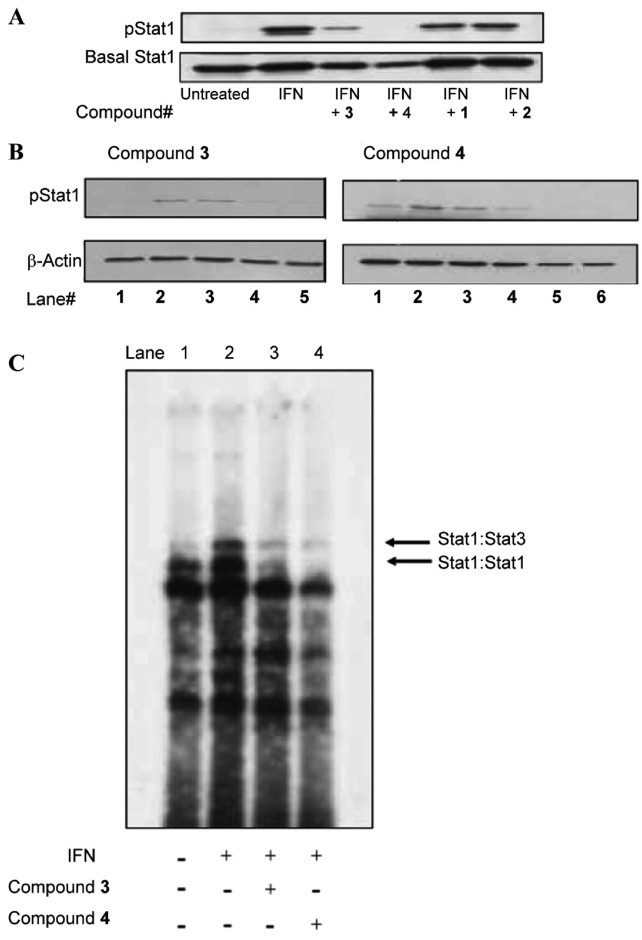

Figure 5. Antagonistic effects of IFN mimetics on IFN-inducible Stat1 phosphorylation. (A) Daudi cells were either left untreated or treated with IFN alfacon-1 in the absence or in the presence of compounds **3**, **4**, **1**, and **2** for 15 min. (B) In dose–response assays, cells were either left untreated (lane 1), treated with IFN alfacon-1(lane 2) or IFN alfacon-1 plus varying doses of **3** (IFN+20, IFN+50 and IFN+80 μM in lanes 3–5, respectively) and **4** (IFN+20, IFN+50, IFN+80 and IFN+100 μM in lanes 3–6, respectively) and the extent of Stat1 phosphorylation determined as per panel A. β-Actin served as the loading control. (C) Daudi cells were either left untreated (−) (lane 1) or treated with IFN alfacon-1 (+) (lane 2) in the presence of compound **3** (lane 3) or **4** (lane 4) for 15 min, as indicated. Nuclear extracts were prepared, mixed with radiolabeled pIRE, resolved by native agarose gel electrophoresis, then the pIRE-bound Stat complexes visualized by autoradiography, as shown.

In a first series of experiments, we examined the effects of all synthesized compounds on the phosphorylation activation of Stat1 in Daudi lymphoblastoid cells. In time course studies (5–30 min), our data revealed that none of the compounds induced the phosphorylation of Stat1 on tyrosine residues (data not shown). Next, because we predicted that these compounds may interfere with IFN alfacon-1 binding to IFNAR, we examined the influence of these compounds on IFN-inducible Stat1 phosphorylation. The data in Figure 5A,B demonstrate that compounds **3** and **4** inhibit the IFN-inducible phosphorylation of Stat1, in a dose-dependent manner. In subsequent studies, focusing on compounds **3** and **4**, we examined whether they would exhibit a similar inhibitory effect on the DNA-binding activity of IFN-inducible Stat1:Stat1 and Stat1:Stat3 complexes. In the electrophoretic mobility shift assays (EMSA) using the pIRE as a probe for Stat complex binding, compounds **3** and **4** reduced IFN-inducible Stat1:Stat1-pIRE and Stat1:Stat3-pIRE complex formation thus antagonizing the effects of IFN at IFNAR (Figure 5C). Viewed altogether, compounds **3** and **4** function as antagonists of IFN−IFNAR interactions.

We disclose here the design of small molecule mimics based on the features of specific surface regions on the IFN, as antagonists for IFNAR. Two regions IRRP-1 and IRRP-3 on the surface of IFN-α2a were used to design the molecular templates de novo. An iterative in silico screening was conducted to design a small focused library of compounds and yielded two moderately potent antagonist molecules. Identification of agonists using structure-based design is the next step in this challenge, and most likely, such agonist molecules may have to consider additional structural features in the design process. Principles disclosed here pave the way to a novel series of small molecules that could potentially be used to design mimics of various functional hotspots on the surface of interferon.

Acknowledgment. This work was supported by a grant from the Canadian Institutes of Health Research (E.N.F. and L.P.K.). L.P.K. is a recipient of an Rx&D HRF-CIHR research career award. An infrastructure grant from the Ontario Innovation Trust provides support for the Molecular Design and Information Technology Centre (MDIT).

Supporting Information Available: ^{1}H NMR, ^{13}C NMR, UV, and HPLC purity data for the synthesized compounds. This material is available free of charge via the Internet at http://pubs.acs.org.

References

(1) Platanias, L. C. Mechanisms of type-I- and type-II-interferon-mediated signalling. *Nat. Rev. Immunol.* **2005**, *5*, 375–386.
(2) Guilhot, F.; Chastang, C.; Michallet, M.; Guerci, A.; Harousseau, J. L.; Maloisel, F.; et al. Interferon α-2b combined with cytarabine versus interferon alone in chronic myelogenous leukemia: French myeloid leukemia study group. *New Engl. J. Med.* **1997**, *337*, 270–271.
(3) Ahmed, A.; Keefe, E. B. Overview of interferon therapy for chronic hepatitis C. *Clin. Liver Dis.* **1999**, *3*, 757–773.
(4) Vedantham, S.; Gamliel, H.; Golomb, H. M. Mechanism of interferon action in hairy cell leukemia: A model of effective cancer biotherapy. *Cancer Res.* **1992**, *52*, 1056.
(5) Billiau, A.; Kieseier, B. C.; Hartung, H. P. Biologic role of interferon beta in multiple sclerosis. *J. Neurol.* **2004**, *251*, 1110–1114.
(6) Lee, P. Y.; Reeves, W. H. Type I interferons as a target of treatment in SLE. *Endocr. Metab. Immune Disord. Drug Targets* **2006**, *6*, 323–330.
(7) Kyogoku, C.; Tsuchiya, N. A compass that points to lupus: Genetic studies on type I interferon pathway. *Genes Immunol.* **2007**, *8*, 445–455.
(8) Koutouzov, S.; Mathian, A.; Dalloul, A. Type I interferons and systemic lupus erythematosus. *Autoimmun. Rev.* **2006**, *5*, 554–562.
(9) Cohen, B.; Novick, D.; Barak, S.; Rubinstein, M. *Mol. Cell. Biol.* **1995**, *15*, 4208–4214.
(10) Mogensen, K. E.; Lewerenz, M.; Reboul, J.; Lutfalla, G.; Uze, G. The type I interferon receptor: Structure, function and evolution of a family business. *J. Interferon Cytokine Res.* **1999**, *19*, 1069–1098.
(11) Kumaran, J.; Wei, L.; Kotra, L. P., Fish, E. N. A structural basis for interferon-α-receptor interactions. *FASEB J.* **2007**, *21*, 3288–3296.
(12) Chill, J. H.; Nivasch, R.; Levy, R.; Albeck, S.; Schreiber, G.; Anglister, J. The human interferon receptor: NMR-based modeling, mapping of the IFN-α2 binding site, and observed ligand-induced tightening. *Biochemistry* **2002**, *41*, 3575–3585.
(13) Chill, J. H.; Quadt, S. R.; Levy, R.; Schreiber, G.; Anglister, J. The human type I interferon receptor: NMR Structure reveals the molecular basis of ligand binding. *Structure* **2003**, *791*, 802.
(14) Platanias, L. C.; Fish, E. N. Signaling pathways activated by interferons. *Exp. Hematol.* **1999**, *27*, 1583–1592.
(15) Kalvakolanu, D. V. Alternate interferon signaling pathways. *Pharmacol. Ther.* **2003**, *100*, 1–29.
(16) Fish, E. N. Definition of receptor binding domains in interferon-α. *J. Interferon Res.* **1992**, *12*, 257–266.
(17) Muller, U.; Steinhoff, U.; Ries, L. F. L.; Hemmi, S.; Pavlovic, J.; Zinkernagel, R. M.; Aguet, M. Functional role of type I and II interferons in antiviral defense. *Science* **1994**, *264*, 1918–1921.
(18) Yohannes, D. Disruption of protein−protein interactions. *Annu. Rep. Med. Chem.* **2003**, *38*, 295–304.

(19) Cochran, A. G. Antagonists of protein−protein interactions. *Chem. Biol.* **2000**, *7*, R85–R94.
(20) Boger, D. L.; Deshrnais, J.; Capps, K. Solution-phase combinatorial libraries: Modulating cellular signalling by targeting protein−protein or protein−DNA interactions. *Angew. Chem., Int. Ed.* **2003**, *4138*, 4176.
(21) Tan, C.; Wei, L.; Ottensmeyer, F. P.; Goldfine, I.; Yip, C. C.; Batey, R. A.; Kotra, L. P. Structure-based de novo design of ligands using a three-dimensional model of the insulin receptor. *Bioorg. Med. Chem. Lett.* **2004**, *14*, 1407–1410.
(22) Roisman, L. C.; Piehler, J.; Trosset, J.-Y.; Scheraga, H. A.; Schreiber, G. Structure of the interferon−receptor complex determined by distance constraints from double-mutant cycles and flexible docking. *Proc. Natl. Acad. Sci. U.S.A.* **2001**, *98*, 13231–13236.
(23) Klaus, W.; Gsell, B.; Labhardt, A. M.; Wipf, B. The three-dimensional high resolution structure of human interferon α-2a determined by heteronuclear NMR spectroscopy in solution. *J. Mol. Biol.* **1997**, *274*, 661–675.
(24) Waine, G. J.; Thymms, M. J.; Brandt, E. R.; Cheetham, B. F.; Linnane, A. W. Structure−function study of the region encompassing residues 26–40 of human interferon-α4: Identification of residues important for antiviral and antiproliferative activities. *J. Interferon Res.* **1992**, *12*, 43–48.
(25) Korn, A. P.; Rose, D. R.; Fish, E. N. Three-dimensional model of a human interferon-α consensus sequence. *J. Interferon Res.* **1994**, *14*, 1–9.
(26) Unity software program from Tripos Inc. (St. Louis, MO) was used to conduct database searches, in conjunction with Sybyl molecular modeling program. Searches were conducted on an Octane2 dual processor computer or a 44-processor Onyx3800 supercomputer.
(27) CAS Registry No. for compound **42**, 903633-37-4, and for compound **44**, 671188-22-0. All the hit compounds were extracted from either NCI Database, LeadQuest Database or Maybridge database, and these were obtained as part of the UNITY software version 4.0, Tripos Inc., St. Louis, MO.
(28) Schinazi, R. F.; Strekowski, L. Unfused heteropolycyclic compounds as visucides, especially against human immunodeficiency virus. PCT/WO 8911279, 1989.
(29) Masters, J.; Hinek, A. A.; Uddin, S.; Platanias, L. C.; Zeng, W. Q.; McFadden, G.; Fish, E. N. Poxvirus infection rapidly activates tyrosine kinase signal transduction. *J. Biol. Chem.* **2001**, *276*, 48371–48375.
(30) Ghislain, J. J.; Fish, E. N. Application of genomic DNA affinity chromatography identifies multiple interferon-alpha-regulated Stat2 complexes. *J. Biol. Chem.* **1996**, *271*, 12408–12413.
(31) Strekowski, L.; Harden, D. B.; Grubb, W. B.; Patterson, S. E.; Czarny, A.; Mokrosz, M. J.; Cegla, M. T.; Wydra, R. L. Synthesis of 2-chloro-4,6-di(heteroaryl)pyrimidines. *J. Heterocycl. Chem.* **1990**, *27*, 1393–1400.
(32) Strekowski, L.; Wilson, W. D.; Mokrosz, J. L.; Mokrosz, M. J.; Harden, B. D.; Tanious, F. A.; Wydra, R. L.; Crow, S. A. Quantitative structure−activity relationship analysis of cation-substituted polyaromatic compounds as potentiators (amplifiers) of bleomycin-mediated degradation of DNA. *J. Med. Chem.* **1991**, *34*, 580–588.
(33) Wilson, W. D.; Strekowski, L.; Tanious, F. A.; Watson, R. A.; Mokrosz, J. L.; Strekowska, A.; Webster, G. D.; Neidle, S. Binding of unfused aromatic cations to DNA—The influence of molecular twist on intercalation. *J. Am. Chem. Soc.* **1988**, *110*, 8292–8299.
(34) Bernatowicz, M. S.; Wu, Y.; Matsueda, G. R. 1*H*-Pyrazole-1-carboxamidine hydrochloride: An attractive reagent for guanylation of amines and its application too peptide synthesis. *J. Org. Chem.* **1992**, *57*, 2497–2502.
(35) Brierley, M. M.; Fish, E. N. Stats: Multi-faceted regulators of transcription. *J. Interferon Cytokine Res.* **2005**, *25*, 733–744.

JM701182Y